

Level Variations in the Caspian Sea under Different Climate Conditions by the Data of Simulation under CMIP6 Project

A. V. Kislov^{a, b, *} and P. A. Morozova^c

^a Faculty of Geography, Moscow State University, Moscow, 119991 Russia

^b Water Problems Institute, Russian Academy of Sciences, Moscow, 119333 Russia

^c Institute of Geography, Russian Academy of Sciences, Moscow, 119017 Russia

*e-mail: avkislov@mail.ru

Received April 1, 2021; revised June 8, 2021; accepted June 10, 2021

Abstract—Water balance components for the territory of the Volga basin and Caspian Sea water area have been analyzed using the results of climatic simulation under CMIP6 Project for reproducing the modern (1859–2014) and preindustrial (~1850) climate, as well as the climate of Holocene optimum (6 thousand years ago) and the Last Glacial Maximum (21 thousand years ago). Volga runoff for the modern and preindustrial periods has been reproduced by models close enough to its actual values, while its components (precipitation and evaporation) have been overestimated. The analysis of the distribution functions of precipitation and evaporation in the Caspian Basin has shown the fluctuations of precipitation to contribute more to the natural variability of the Caspian level. A probability distribution function of possible fluctuations of the Caspian Sea was derived based on the theory of Brownian motion.

Keywords: the Caspian Sea, natural variations, stochastic analysis

DOI: 10.1134/S0097807821060099

INTRODUCTION

The climatic models (Earth system models) are complex mathematical constructions describing the thermodynamics of the atmosphere and ocean, cryosphere, land properties, biogeochemical cycles, and vegetation cover.

The world community regularly compares different climate models. The best known project is CMIP (Coupled Model Intercomparison Project), the sixth phase of which (CMIP6) [17] is being implemented now, including coordinated experiments following common protocols.

Such experiments are used to assess the operation quality of models in reproducing the modern climate and the sensitivity of the models to changes in boundary conditions. The following experiments are obligatory for each participant:

a test experiment, aimed to reproduce the preindustrial state of the climate (corresponding to the mid-XIX century);

a historical experiment, reproducing the climate of the period 1850–2014;

an experiment with an instantaneous fourfold increase in carbon dioxide concentration relative to the preindustrial level, the duration is 150 model years;

an experiment with an increase in carbon dioxide concentration by 1% per year relative to the preindustrial level, the duration is 150 model years;

experiments with prescribed state of the ocean, sea ice distribution, and the gas composition of the atmosphere, which are specified based on observation data for 1979–2014.

Many other experiments are also used to study the sensitivity of models to different forcings, reproducing possible scenarios of future climate changes, the climates of the past, aimed to assess the operation quality of individual components of the climate model.

In this study, data of some CMIP6 experiments are used to study the water balance of the Caspian Sea and its level variations. In any climate model, the module describing the properties of land is based on a regular grid consisting of cells covering the entire Earth land surface, with cell sizes varying from one (in regional models) to tens of kilometers. Each cell is characterized by the hydrophysical parameters of its surface, describing, as a necessary element, the properties of the land associated with the presence of water bodies (lakes) in them. Some lakes, which are relatively small, lie within the cell, while the description of larger lakes requires coordinated data in several cells. The description of lakes is required primarily to adequately characterize the effect on the atmosphere due to water vapor and heat fluxes and the surface roughness and

albedo. In some cases, parallel to the incorporation of the contribution of lakes to the state of the atmosphere, the problem of reproducing the properties of the lake itself is also solved.

The problem is complex because of the number of lakes being large and their sizes varying within wide limits. This requires their detection by grid databases with cells of different sizes [12, 15]. The overwhelming majority of lakes are not reproduced in climatic models as individual objects with unique natural and hydrological characteristics. In most cases, the properties of the surface, specified in a database, reflect cells (or their parts) occupied by water (with a constant storage not reflecting variations in the lake water balance). This is enough to describe water evaporation within land massifs and to reproduce the specifics of heat exchange with the atmosphere. In some cases, the water body is supplemented by a simple algorithm to account for the two-layer structure of deep lakes to better reproduce the specifics of the thermal regime of their surface.

However, the problems of simulation are due not only to the identification of water bodies, but to errors in the reproduction of their characteristics by atmospheric models. The fact is that the quality of simulation is strongly dependent on the size of the object. This is due to the natural effect of a decrease of the error at summing model data over large areas. Therefore, an extended object, represented by many model cells, can be reproduced in a numerical experiment much better than a small object [25]. This implies that the analysis of the largest water objects on the land is in principle more reliable. The Caspian Sea is such an object. Note that, in the relatively recent geological past, the Black Sea was an analogous object, when, during glaciation maximum (21 thous. years ago) and in the post-glacial period, its level was several tens of meters below the Bosphorus, a fact which, at level drop in the World Ocean, led to the isolation of the basin and its transformation into a drainless water body with the appropriate regime of level variations [21].

When water bodies as large as those are simulated, the consideration of their internal dynamics may be of importance. Far from all climatic models specify the Caspian Sea as *the sea* in the configuration of grid cells and use the appropriate oceanic calculation module. However, even if such description is included in the model (as it was made in the models of Laplace Institute (France), Institute of Numerical Mathematics (Russia), and others), the size of the model sea is not controlled by water balance and the level remains constant.

Under such conditions, the problem of level variations in the Caspian Sea (a sea that is not presented in the model) can be solved only by an indirect method through the calculation of all water balance components in the drainage area and the sea water area,

implying by the latter the group of cells which represents its water surface in the model.

Experiments and Models

The object of analysis was the model data of climatic experiments carried out under CMIP6 and available from [19] for four experiments: a control experiment (piControl), a historical experiment, as well as experiments aimed to reproduce the climate of mid-Holocene (midHolocene) and the conditions of the so-called maximum of the last glaciation (Last Glacial Maximum). For brevity, they are denoted below as PI, H, mH, LGM.

The protocol of the experiments is given in [16]. PI is among the basic experiments in CMIP6, in which the boundary conditions and the parameters corresponding to the preindustrial epoch are specified unchanged for the entire calculation period (data for 1850 are used). In the case of H, simulation from 1850 to 2014 is made with a varying parameter set (the solar constant, the concentrations of greenhouse gases and aerosols, including the volcanic aerosol), based on data of measurements for this period.

The experiments mH and LGM, involving the reproduction of past climates (CMIP6-PMIP4), are described in detail in [20, 29]. They are aimed to simulate the sections 6 and 21 thousand calendar years ago, which are canonic for paleoclimatology and characterize the conditions in the interglacial and glacial epochs. To do this, the gas composition of the atmosphere and the orbital parameters are specified in both experiments in accordance with the data of reconstruction, resulting in a change in the distribution of solar energy reaching the surface. In the experiment mH, this exhausts the specified external effects. The results of this experiment are reviewed in [13]. The key features of the experiment LGM include the simulation of climate as a response to a decrease in CO₂ concentration, the overall increase in the volumes of glaciation, the appearance of sheet glaciers in the territory of Eurasia and North America, a drop in the World Ocean level (down to -115...-130 m below sea level), and change of the land/sea configuration.

Note that the experiments PI, mH, and LGM consisted in calculations aimed to study the steady, equilibrium state, while the experiment H is a nonstationary experiment made to reflect the current response of the climate system to background changes, primarily, to the increase in greenhouse gases in the atmosphere.

The problems in this study were solved with the use of data of four models (Table 1), for which the database contains all required simulation results. The thing is that CMIP6 is still not completed and the content of the database is extending.

Volga runoff, as well as the evaporation and precipitation in its basin were calculated using the modern configuration of the Volga basin interpolated into

Table 1. Brief characteristics of climate models

Model name	Short denotation in the article	The number of cells along longitude × the number of cells along latitude	Experiment duration, years*	References
AWI-ESM-1-1-LR	awi	192 × 96	piControl—100 historical—165 midHolocene—100 lgm—100	[30]
INM-CM4-8	inm	180 × 120	piControl—531 historical—165 midHolocene—200 lgm—200	[31]
MIROC-ES2L	miroc	128 × 64	piControl—500 historical—165 midHolocene—100 lgm—100	[18]
MPI-ESM1-2-LR	mpi	192 × 96	piControl—1000 historical—165 midHolocene—100 lgm—100	[28]

* According to [19].

model grids. The characteristics of apparent evaporation (the difference between evaporation and precipitation) over the Caspian water area were calculated with the use of the cells where the option *sea* was chosen in the land/sea mask for the territory under consideration. In the miroc model, the Caspian Sea was not specified in model mask as *sea*; therefore, the cells belonging to it were chosen by the authors from the total data by the large evaporation sums that were several times greater than the values in the neighboring cells.

Analysis of the Averaged Values and the Probability Distribution Functions of Water Balance Components

We will start the analysis of the simulation data by comparing the mean values of water balance components (averaged over the basin and over the period of computer experiment). First, we compared the data of experiments, which, by their nature, could be compared with the climatic (modern) data. Based on paleogeographic concepts and the conditions of the implementation of experiments PI, Mh, and H (as mentioned above), the data that refer to the modern climate and the mid-Holocene are to be in general agreement as they refer to the interglacial stage. The differences that can be seen, for example, in the Blytt–Sernander paleogeographic scheme are much less important than the difference between glacial/interglacial epochs.

As can be seen from Fig. 1, all four models demonstrate similar behavior: the model precipitation and evaporation over the Volga basin are considerably

overestimated (by 25–60 and 60–100%, respectively) compared with the modern data; however, despite these discrepancies, the runoff values were close to the hydrometric runoff values (the scatter was $\pm 30\%$). This fact causes contradictory impressions. On the one hand, the absolute value of river runoff is reproduced more or less adequately. On the other hand, this is the result of the incorrect reproduction of precipitation and evaporation by the model because of the incorrect simulation of the features of the regional climate regime. This fact reduces the level of confidence in the simulation results, because the observed incorrect reproduction of the runoff-formation mechanism does not guarantee the correctness of the results under climate conditions other than the modern ones. As far as the products of global modeling are involved, theoretically, the situation can be improved by reanalysis or, moreover, current data of weather forecast (see below), the use of which always “forces” the model onto the correct evolution trajectory.

Comparing the precipitation and evaporation over the Volga Basin, as well as the apparent evaporation, we note that the probability distribution functions can be very well approximated by the normal distribution. One can clearly see that the variation ranges are different and the variations of precipitation are much greater (Fig. 2).

To control the runoff value, directly calculated by the models, it was compared with the so-called climatic runoff, which is also calculated by model data. The latter value is calculated as the difference between precipitation and evaporation over the basin, which is averaged over the entire observation period. Consider-

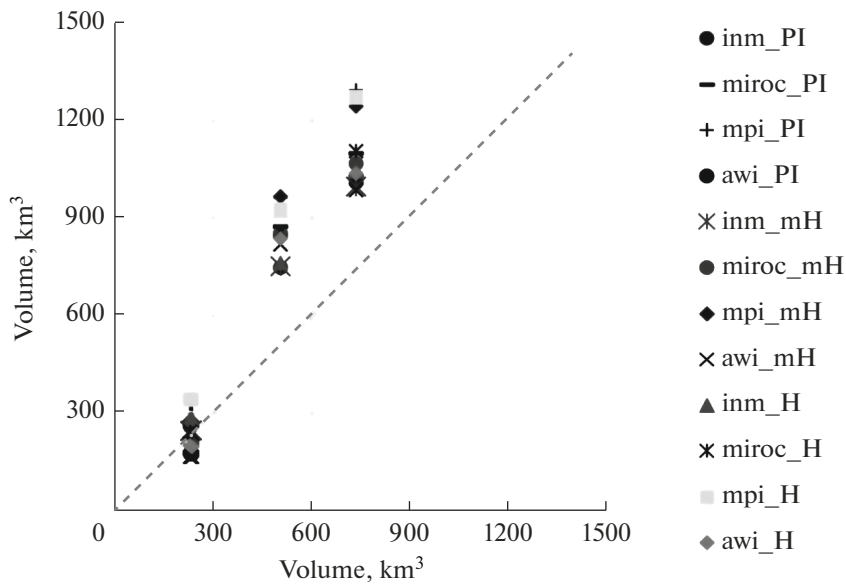


Fig. 1. Comparison (by data of observation and simulation) of data on precipitation, evaporation, and runoff (km³) over the Volga basin by data of climatic models. Observation data: runoff, evaporation, and precipitation [2, 4] are plotted successively on the abscissa.

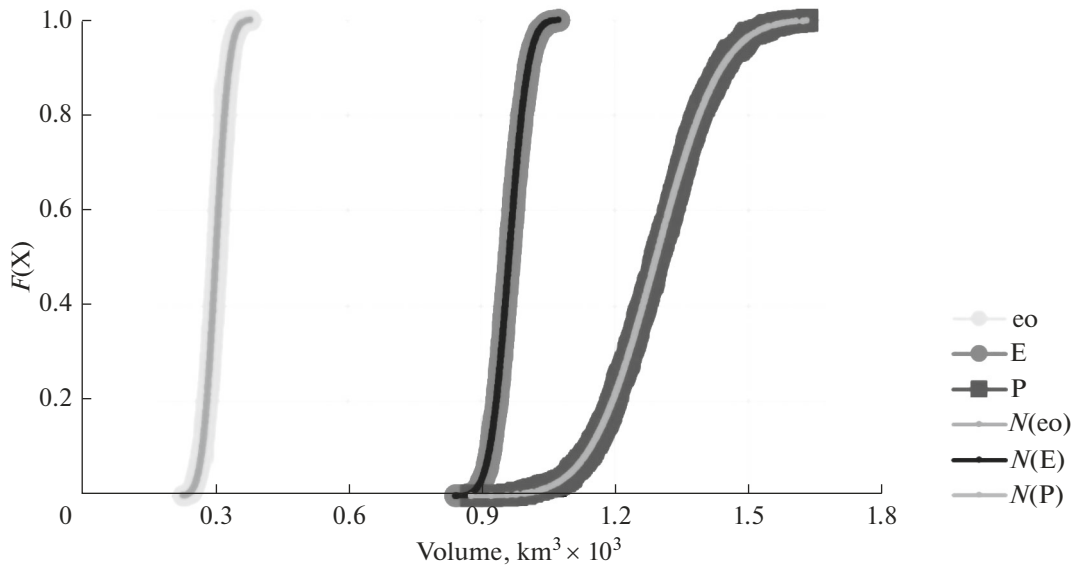


Fig. 2. Integral distribution functions of the recurrence of precipitation and evaporation, averaged over Volga basin, as well as apparent evaporation from sea surface (10⁻³ km³) for experiment mpi_PI and the appropriate functions of normal distribution.

ing the algorithm used for the model calculations, we can expect the equality of the runoff and the climatic runoff; however, as can be seen from Table 2, some moisture accumulations/losses are possible in the soil layer. Overall, the deviations never exceed 2%, except for one case corresponding to experiment inm_LGM. However, the excess over the climatic runoff in this case is due to the incorporation of the additional

amount of water that penetrates into the Volga Basin because of melting of the Scandinavian Glacial Sheet.

Equation Describing the Dynamics of Caspian Sea Level

The water balance is described by the equation:

$$\frac{dV}{dt} = Q_{in} - Q_{out}. \tag{1}$$

Table 2. Comparison of the runoff Q calculated by the models with the climatic runoff Q_c

Observations and experiments	$Q - Q_c, \text{ km}^3$	$(Q - Q_c)/Q_c$
obs	5	0.021
inm_PI	1.1	0.004
miroc_PI	-3.4	-0.015
mpi_PI	-2.2	-0.007
awi_PI	-2.2	-0.013
inm_H	0.3	0.001
miroc_H	-5.5	-0.023
mpi_H	-2.7	-0.008
awi_H	-3.4	-0.017
inm_mH	2.3	0.009
miroc_mH	-5.5	-0.026
mpi_mH	-3.0	-0.011
awi_mH	-1.3	-0.008
inm_LGM	11.0	0.079
miroc_LGM	-3.5	-0.017
mpi_LGM	-3.0	-0.019
awi_LGM	-2.4	-0.015

The input component of the budget is determined by river flow (the subsurface component is <10% (in fact, 1% [9]). On the average, ~80% (90% is possible for some stages) of river runoff is due to the Volga River runoff Q , i.e., $Q_{in} = Q/k$, $k = 0.8$, $Q_{out} \equiv e$, i.e., the difference “evaporation minus precipitation” for water surface. This also includes water inflow into Kara-Bogaz-Gol Bay and its further evaporation. Observations show that, on the average, the inflow and the outflow values are similar; therefore, the variations of water volume (sea surface area and level) are commonly a result of a minor disbalance. When the background values of water balance components change, the sea tends to find new equilibrium level and area [1]. Under such stationary conditions, we have from (1)

$$\frac{Q_0}{k} = e_0. \quad (2)$$

Let us check whether the condition (2) holds for model data. Clearly, this condition is fictitious in this case as the water cycle does not have to be balanced.

First, we choose for checking the data taken from numerical experiments H, PI, mH. Table 3 compares the ratios e_0/Q_0 for data of the analyzed models. According to (2) this ratio is to be 1.25. The model data yields ~1 with a minor scatter. In fact, this means that an important relationship exists between water balance components, namely, we can assume that in the models mentioned above the “absent” water balance in the Caspian Sea is supported by the contribution of the Volga alone. The ratio for awi model is on the average ~1.9. This means, under the same assumptions, that the contribution of the Volga accounts for only ~50% of water losses through evaporation from water surface, i.e., here we see an underestimation of the Volga runoff contribution, while the first three models mentioned above overestimate its role.

As to the period of the last glaciation, the situation is more complicated. The thing is that, according to paleogeographic data, a very deep regression was observed in that period [27]. A study of its causes, based on the analysis of simulation data, revealed the leading role of the decrease in the Volga runoff [26]. Among the models considered in this study, two models—mpi and inm—gave analogous quantitative results. Other two models—miroc and awi—demonstrated no decrease in the Volga flow, notwithstanding the considerable decrease in precipitation over Volga Basin because of the parallel decrease in evaporation.

If we exclude from the Caspian Sea water area its northern part, thus trying to take into account the fact of the decrease in the Caspian Sea area during the latest glaciation, this will lead to a decrease in the ratio e_0/Q_0 , calculated by model data: it will be ~1, though the scatter in data of different models will be much greater.

Note that under real conditions, the volume of evaporation from sea surface depends on level variations, because, for example, at its considerable increase relative to the present state, the area of shallow zones increases appreciably, leading to greater

Table 3. Ratios of the apparent evaporation and Volga runoff averaged over the period of experiment

Model, experiment	e_0/Q_0	Model, experiment	e_0/Q_0
mpi_H	0.9	inm_H	1.0
mpi_mH	1.4	inm_mH	1.1
mpi_PI	0.9	inm_PI	1.0
miroc_H	0.9	awi_H	1.7
miroc_mH	1.6	awi_mH	2.0
miroc_PI	1.0	awi_PI	1.9

evaporation. However, the analysis of the hypsometric curve shows that this effect becomes significant starting from the level excess of ≥ 10 m relative to the present values [10]. However, if the range of level variations is not as large as that, this feedback is not significant.

Now we add expressions (1) and (2) (implying that $dV = f dh$, h is sea level, f is sea area) to obtain

$$f \frac{dh}{dt} = \frac{Q_0}{k} \left(\frac{Q - Q_0}{Q_0} - \frac{e - e_0}{e_0} \right). \quad (3)$$

The changes of the area as a function of the level can be described as $f = a + bh$ (with a zero reference point at -28 m), though the coefficients of this equation are somewhat different in the ranges $h \leq -5$, $-5 < h < 0$, $h \geq 0$ m.

However, direct calculations show that, for example, at deviations by ± 5 m, the deviations of the area from its mean are $\leq 10\%$. Therefore, we assume that $dV = f_0 dh$ and after integration, we obtain

$$h - h_0 = \frac{Q_0}{k f_0} \int_0^t \left(\frac{Q - Q_0}{Q_0} - \frac{e - e_0}{e_0} \right) dt. \quad (4)$$

For the present-day values, $Q_0/kf_0 \cong 0.8$ m/year.

The obtained relationship shows that sea level anomalies appear due to the successive accumulation of relative anomalies of river flow and apparent evaporation. According to the data of simulation, the effect of the first factor is dominant, while the contribution of the second summand reaches 20% only in some periods of numerical experiments. This opinion has been repeatedly emphasized [7, 8, 24]. However, studies appeared in which the apparent evaporation was evaluated by reanalyses (GFS, ERA-Interim, JRA, NCEP/NCAR, and NCEP/DOE), as well as by data of real-time weather forecasts [3, 14]. These results are so far contradictory: the use of some bases yields comparable and even dominating role of variations of apparent evaporation, while others do not allow any conclusions to be made at all.

Now, we can use the simulation data to calculate the cumulative sums of the Volga runoff and apparent evaporation and to interpret these results as level variations, supposing (taking into account the assumptions made) that the factor in (4) is close to unit.

The Dynamics of the Caspian Sea Level Retrodicted by Data of Runoff and Apparent Evaporation Variations

First, we consider the data of experiment H (Fig. 3). All models showed the model regime to be sensitive to the progressive rise of the environmental temperature in the XX–XXI. However, the effect of this factor was found to be not sufficient to control atmospheric circulation and the hydrological cycle in European region and the adjacent Asian territory, with the result that the model curves are not similar and do

not agree with the real behavior of the Volga runoff. This demonstrates a typical feature of climate modeling, i.e., the loss of phase agreement. At the same time, we can note that the range of the curves is similar to the variations that have taken place in the Caspian Sea in the recent one and a half century. All curves show epochs of long-term changes with a rate of level rise/drop of 0.4–1.0 m/10 years. More abrupt changes can also be seen. Thus, the awi model demonstrates a decrease in sea level near the mid-XX century, the rate of which is 2.5 times greater than the estimates given above. In this case, variations, including those with large differences between the values, are mostly typical of runoff variations and are mainly due to changes in the precipitation onto the Volga Basin territory. Such variations in the apparent evaporation are much rarer. The importance of such anomalies in the context of the analysis of individual dry years (as, for example, under the conditions of the catastrophic anomaly of the summer 2010) was mentioned in [11]. At the same time, the comparison of the probability distribution functions (Fig. 2) clearly demonstrates that the variation range of the apparent evaporation is much narrower than the variation range of precipitation.

Note that, compared with CMIP5 data [23, 24], the results of CMIP6 considered here show somewhat wider (by 15–20%) variability, which is closer to the real fluctuation range.

However, the interval of 165 years in experiment H (from which the first and the last ~ 20 years, i.e., the characteristic transition times of the Caspian Sea dynamics, are to be excluded before the analysis) is too short to study the behavior of such an inertial object as the Caspian Sea.

In this context, more informative will be the results of long-term simulation PI, the more so that PI experiment was carried out to obtain the steady state. The analysis used the data of three models, because the data for awi model are available only for 100 model years. Their analysis generally confirms the conclusions regarding the length and rates of Caspian level variations, which have been made above in the analysis of the results of experiment H.

Integral-difference curves show different behavior over time. Typical for all models are fluctuations of the values 30–50 years in length with a characteristic range of ~ 2 m. Slower trend-type variations extend over many decades and feature the rates of level variations of ~ 0.6 m/10 years. In this case, the main contribution to level variations is again due to river flow, though deep anomalies can also be seen (although much rarer) in the variations of apparent evaporation.

Let us consider in greater detail the longest, 1000-year series of mpi_PI (Fig. 4). It can be clearly seen to be inhomogeneous. Thus, first, long epochs ~ 250 years long were taking place against the background of low sea level, during which the level first was decreasing and next increasing, but later this gave

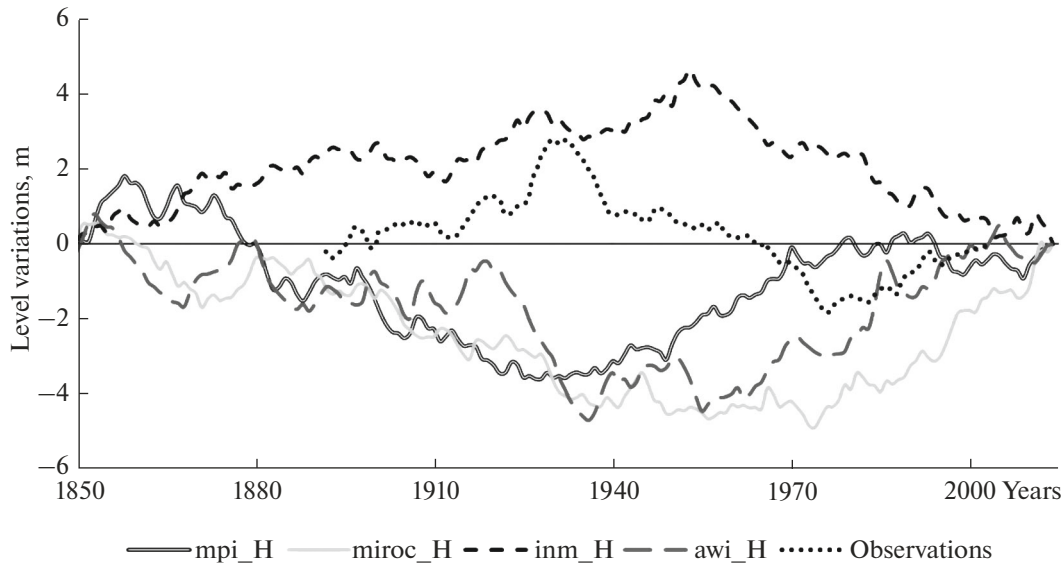


Fig. 3. Integral-difference curves of Volga runoff by data of experiment *Historical* and observation data.

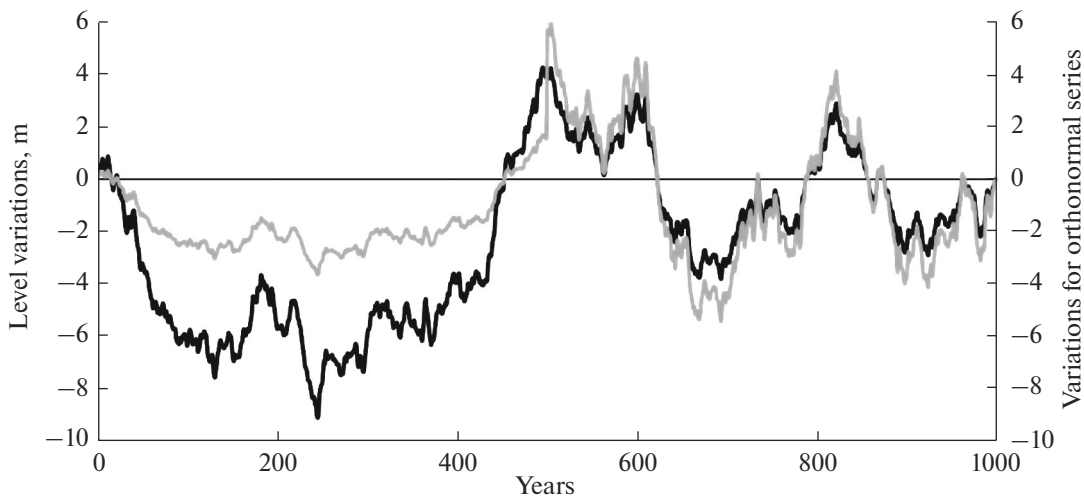


Fig. 4. Integral-difference curves of Volga runoff (black) for experiment *mpi_PI* (m) and (gray) standardized dimensionless values at 2.5 and 0.7 m for the first and second 500-year interval, respectively.

place to rhythmic variations with a period of ~200 years. The empirical histogram (Fig. 5) for such conditions appears to consist of two distribution function.

This type of irregular behavior of the model climate regime (which could be supposed to contradict to the procedure of experiment *PI*, meant especially to reproduce a stationary regime) resembles random fluctuations, the regime of which showed a transformation near about the middle of the model experiment. Nothing can be said about the nature of this transition regime but a general note that it could be an

effect of the secular volatility of the regional climate, existing under globally equilibrium regime.

At the same time, the interpretation of calculations by (4) can be wrong. To prevent this, we can try to avoid using f_0 , but take into account the variations of sea area along with its level variations. Such correction can be introduced in the following way.

If we interpret Caspian level variations as a realization of a random walk of the type of Brownian motion [6], their variance is to be described by the expression

$$\sigma_{hst}^2 = \frac{\tau_q \sigma_q^2}{\lambda}. \quad (5)$$

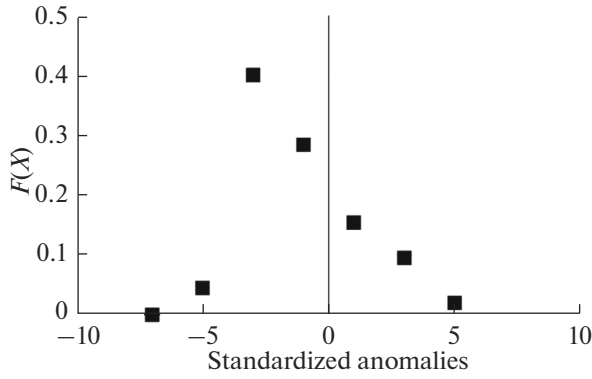


Fig. 5. Empirical histogram of standardized anomalies of Volga runoff (Fig. 4), dimensionless values.

This is a stationary state in which the amplitude of anomalies remains statistically constant.

We assume that the characteristic time of changes is the same as that corresponding to the modern measurements, i.e., we take $\tau_q = 2$ year to avoid year-to-year correlation. The function in the denominator is related, in particular, with the features of the hypsometric curve. In the intervals where the sea level falls below -5 m (measured from -28 m), $\lambda = \lambda_1 = 0.01$ 1/year; in the interval from -5 m to zero, $\lambda = \lambda_2 = 0.05$ 1/year, and at higher levels, $\lambda = \lambda_3 = 0.02$ 1/year. The last factor in the nominator in (5) combines the variances of the fluctuations of flow and apparent evaporation. For the case of the model series under consideration, these are 0.0025 and 0.0045 (m/year)², respectively; therefore $\sigma_q^2 = 0.007$ (m/year)². Note that the variance of flow fluctuations is an order of magnitude less than that derived from modern observations [5]. In the first ~ 500 years of experiment mpi_PI it is reasonable to assume $\lambda = 0.01$ 1/year, while in the next ~ 500 years, we take the mean value between λ_2 and λ_3 , i.e., 0.035 1/year. With such assumptions, we have $\sigma_{hst} = 2.5$ m for the first interval and $\sigma_{hst} = 0.7$ m for the second one.

We will use these values to standardize the anomalies of sea level. After that, the characteristics of the first and second 500-year intervals becomes more similar (Fig. 4), i. e., the incorporation of the morphological features of the basin somewhat reduced the heterogeneity of the series.

We go further along this line and pass to the construction of the probability density for the fluctuations of Caspian Sea level. Its theoretical form was obtained under the assumption that the level dynamics is described by an equation in which the assimilation of incoming water and the evaporation from water surface are taking place in a basin of a certain shape, determined by the hypsometric curve [22]

$$p = p_0 \exp\left(-\frac{(h-h_0)^2}{2D/\lambda}\right), \left\{ \begin{array}{l} \lambda = \lambda_1, \quad h \leq \xi \\ \lambda = \lambda_2, \quad \xi < h < \eta \\ \lambda = \lambda_3, \quad h \geq \eta \end{array} \right\}. \quad (6)$$

Here D/λ characterizes the variance: $D = \tau_q \sigma_q^2$ (see formula (5)), $\xi = -5$ m and $\eta = 0$ m are inflection points on the hypsometric curve: the values of λ , corresponding to intervals of h , are given below. The constant p_0 is determined from the expression

$$\frac{1}{P_0} = \int_{-\infty}^{\xi} \exp\left(-\frac{(h-h_0)^2}{2D/\lambda_1}\right) dh + \int_{\xi}^{\eta} \exp\left(-\frac{(h-h_0)^2}{2D/\lambda_2}\right) dh + \int_{\eta}^{\infty} \exp\left(-\frac{(h-h_0)^2}{2D/\lambda_3}\right) dh. \quad (7)$$

Let us return to experiment mpi_PI. For the series consisting of standardized values $D = 1$, and the average value for the entire 1000-year series is $h_0 = -1.1$ m. An analytical expression for integrals in (7) cannot be obtained; therefore, their values were calculated with the use of the well-known “Tables of the Values of Laplace Function.” The calculations yielded $p_0 = 0.4$, and the function sought for represents a nearly symmetrical single-mode curve.

The empirical hystogram (Fig. 5) differs from it by a characteristic skew toward negative anomalies. This is due to the above-mentioned heterogeneity of the initial model integral-difference series (Fig. 4), which has been reduced but not eliminated completely.

CONCLUSIONS

Data of climatic simulation were used to analyze level variations of the Caspian Sea in different epochs. Such estimates can be obtained only indirectly, because the sea is not described in the models as an object of water balance of river runoff and apparent evaporation, but is represented in the territory by cells covered by water. The result was the forced assumption that level variations are directly described by integral-difference curves of Volga runoff and apparent evaporation.

As the result, it was found that climate models reproduce the variations of the decade and secular scale with an amplitude close to the actual one; however, the comparison of the simulated and observed phases of these variations (for the recent 165 years) showed their complete disagreement (this is also true for the difference between the models). In this case, while the values of the Volga runoff are reproduced by the model with at least some similarity, the runoff components (precipitation and evaporation averaged over Volga basin) are largely overestimated. This suggests that the characteristics of atmospheric circulation, the regime of precipitation, evaporation, and

snow accumulation, reproduced by the models are far from reality. Taking this into account, we note that the prospects of forecasting Caspian Sea level to the XXI century based on data of climate simulation CMIP are very poor.

An important feature of the long 1000- or 500-year experiments PI was the heterogeneity of the level regime, reconstructed by the data of variations of the Volga runoff and apparent evaporation. This heterogeneity manifests itself in long epochs (~500 years) with different behavior of the simulate characteristics. This is somewhat surprising, because the experiment PI has been especially organized with external impacts specified constant all over its duration in order to obtain a reproduction of stable climate regime. Such procedure seems not to guarantee the stationarity of the regional climate regime. It is also not clear how long is to be the model experiment to ensure such stationarity, and whether such stationarity is achievable in principle.

This fact demonstrates that there are no reasons to expect that relatively short model experiments mH and LGM provide reliable data on decade and secular variations of regional climate. At the same time, the data of paleosimulation convincingly demonstrate that there were no conditions for the formation of superlarge anomalies (with Caspian level amplitudes of several meters). Therefore, their genesis lies beyond the common climatic–hydrological fluctuations, and specific factors are to be taken into account.

FUNDING

The work of A.V. Kislov was supported by the Russian Science Foundation, project no. 19-17-00215; the work of P.A. Morozova was carried out under Governmental Order 0148-2019-0009.

REFERENCES

1. Bogoslovskii, B.B., *Ozerovedenie* (Limnology), Moscow: Mosk. Gos. Univ., 1960.
2. *Vodnyi balans i kolebaniya urovnya Kaspiiskogo morya. Modelirovanie i prognoz* (Water Balance and Level Variations in the Caspian Sea), Moscow: Triada ltd., 2016.
3. Vyruchalkina, T.Yu., Dianskii, N.A., and Fomin, V.V., Effect of long-term variations in wind regime over Caspian Sea Region on the evolution of its level in 1948–2017, *Water Resour.*, 2020, vol. 47, no. 2, pp. 348–358.
4. *Gidrometeorologicheskie aspekty problemy Kaspiiskogo morya i ego basseina* (Hydrometeorological Aspects of the Problem of the Caspian Sea and its Basin), Shiklomanov, I.A. and Vasil'ev, A.S., Eds., St. Petersburg: Gidrometeoizdat, 2003.
5. Golitsyn, G.S., Ratkovich, D.Ya., Fortus, M.I., and Frolov, A.V., On the present-day rise in the Caspian Sea level, *Water Resour.*, 1998, vol. 25, pp. 117–122.
6. Demchenko, P.F. and Kislov, A.V., *Stokhasticheskaya dinamika prirodnykh ob'ektov* (Stochastic Dynamics of Natural Objects), Moscow: GEOS, 2010.
7. Kosarev, A.N., Kuraev, A.V., and Nikonova, R.E., Modern hydrological conditions in the Northern Caspian Sea, *Vestn. Mosk. Univ., Ser. 5: Geogr.*, 1996, no. 5, pp. 47–53.
8. Mikhailov, V.N. and Povalishnikova, E.S., Once again about the causes of Caspian Sea level variations in the XX century, *Vestn. Mosk. Univ., Ser. 5: Geogr.*, 1998, no. 3, pp. 47–53.
9. Panin, G.N., Mamedov, R.M., and Mitrofanov, I.V., *Sovremennoe sostoyanie Kaspiiskogo morya* (The Current State of the Caspian Sea), Moscow: Nauka, Inst. Vodn. Probl., RAN, 2005.
10. Frolov, A.V., DSM-simulation of long-term level variations in the Caspian Sea in paleotime. www.iwp.ru/about/news/v-ivp-ran-proshel-onlayn-seminar-po-kaspiyu/.
11. Arpe, K., Leroy, S., Lahijani, H., and Khan, V., Impact of the European Russia drought in 2010 on the Caspian Sea level, *Hydrol. Earth Systems Sci.*, 2012, vol. 16, pp. 19–27.
12. Baracchini, T., Chu, P.Y., Sukys, J., Lieberherr, G., Wunderle, S., Wuest, A., and Bouffard, D., Data assimilation of *in situ* and satellite remote sensing data to 3D hydrodynamic lake models: a case study using Delft3D-FLOW v4.03 and OpenDA v2.4, *Geosci. Model Dev.*, 2020, vol. 13, pp. 1267–1284.
13. Brierley, C.M., Zhao, A., Harrison, S.P., Braconnot, P., Williams, C.J.R., Thornalley, D.J.R., Shi, X., Peterschmitt, J.-Y., Ohgaito, R., Kaufman, D.S., Kageyama, M., Hargreaves, J.C., Erb, M.P., Emile-Geay, J., D'Agostino, R., Chandan, D., Carre, M., Bartlein, P.J., Zheng, W., Zhang, Z., Zhang, Q., Yang, H., Volodin, E.M., Tomas, R.A., Routson, C., Peltier, W.R., Otto-Bliesner, B., Morozova, P.A., McKay, N.P., Lohmann, G., Legrande, A.N., Guo, C., Cao, J., Brady, E., Annan, J.D., and Abe-Ouchi, A., Large-scale features and evaluation of the PMIP4-CMIP6 midHolocene simulations, *Clim. Past*, 2020, vol. 16, pp. 1847–1872.
14. Chen, J.L., Pekker, T., Wilson, C.R., Tapley, B.D., Kostianoy, A.G., Cretaux, J.-F., and Safarov, E.S., Long-term Caspian Sea level change, *Geophys. Res. Lett.*, 2017, vol. 44, pp. 6993–7001.
15. Choulga, M., Kourzeneva, E., Balsamo, G., Boussetta, S., and Wedi, N., Upgraded global mapping information for earth system modelling: an application to surface water depth at the ECMWF, *Hydrol. Earth Syst. Sci.*, 2019, vol. 23, pp. 4051–4076.
16. Earth System Documentation. <https://view.es-doc.org/index.html?renderMethod=id&project=cmip6&id=8c42ab001ef2-4d5b-ade1-8bf8803cb6d4> (accessed March 5, 2021).
17. Eyring, V., Bony, S., Meehl, G.A., Senior, C.A., Stevens, B., Stouffer, R.J., and Taylor, K.E., Overview of the Coupled Model Intercomparison Project Phase 6 (CMIP6) experimental design and organization, *Geosci. Model Dev.*, 2016, pp. 1937–1958.
18. Hajima, T., Watanabe, M., Yamamoto, A., Tatebe, H., Noguchi, M.A., Abe, M., Ohgaito, R., Ito, A., Yamazaki, D., Okajima, H., Ito, A., Takata, K., Ogochi, K., Watanabe, S., and Kawamiya, M., Development of the MIROC-ES2l Earth system model and the evaluation of biogeochemical processes and feed-

- backs, *Geosci. Model Dev.*, 2020, vol. 13, pp. 2197–2244.
19. <https://esgf-node.llnl.gov/search/cmip6/> (Accessed: March 5, 2021).
 20. Kageyama, M., Albani, S., Braconnot, P., Harrison, S.P., Hopcroft, P.O., Ivanovic, R.F., Lamber, F., Marti, O., Peltier, W.R., Peterschmitt, J.-Y., Roche, D.M., Tarasov, L., Zhang, X., Brady, E.C., Haywood, A.M., LeGrand, A.N., Lunt, D.J., Mahowald, N.M., Mikolajewicz, U., Nisancioglu, K.H., Otto-Bliesner, B.L., Renssen, H., Tomas, R.A., Zhang, Q., AbeOuchi, A., Bartlein, P.J., Cao J., Li, Q., Lohmann, G., Ohgaito R., Shi X., Volodin, E., Yoshida, K., Zhang, X., and Zheng, W. The PMIP4 contribution to CMIP6, Pt 4, Scientific Objectives and Experimental Design of the PMIP4-CMIP6 Last Glacial Maximum Experiments and PMIP4 Sensitivity Experiments, *Geosci. Model Dev.*, 2017, vol. 10, pp. 4035–4055.
 21. Kislov, A., On the interpretation of century-millennium-scale variations of the Black Sea level during the first quarter of the Holocene, *Quaternary Int.*, 2018, vol. 465, pp. 99–104.
 22. On the probability distribution of sea level changes in the Caspian Sea, *Pure Appl. Geophys.*, 2020, vol. 177, pp. 5943–5949.
 23. Kislov, A.V., The interpretation of secular Caspian Sea level records during the Holocene, *Quaternary Int.*, 2016, vol. 409, pp. 39–43.
 24. Kislov, A.V., Panin, A., and Toropov, P., Current status and palaeostages of the Caspian Sea as a potential evaluation tool for climate model simulations, *Quaternary Int.*, 2014, vol. 345, pp. 48–55.
 25. Kislov, A., Tarasov, P.E., and Sourkova, G.V., Pollen and other proxy-based reconstructions and PMIP simulations of the last glacial maximum mean annual temperature: an attempt to harmonize the data-model comparison procedure, *Acta Palaeontol. Sin.*, 2002, vol. 41, pp. 539–545.
 26. Kislov, A. and Toropov, P., Modeling extreme Black Sea and Caspian Sea levels of the past 21 000 years with general circulation models in *Geology and Geoarchaeology of the Black Sea Region: Beyond the Flood Hypothesis: Geological Society of America Special Paper*, Buynevich, I.V. and Yanko-Hombach, V., Gilbert, A.S., Martin, R.E., Eds., 2011, vol. 473, pp. 27–32.
 27. Krijgsman, W., Tesakov, A., Yanina, T., et al., Quaternary time scales for the Pontocaspian domain: Interbasinal connectivity and faunal evolution, *Earth-Sci. Rev.*, 2019, vol. 188, pp. 1–40.
 28. Mauritsen, T., Bader, J., Becker, T., Behrens, J., Bitner, M., Brokopf, R., Brovkin, V., Claussen, M., Crueger, T., Esch, M., Fast, I., Fiedler, S., Flaschner, D., Gayler, V., Giorgetta, M., Goll, D.S., Haak, H., Hagemann, S., Hedemann, C., Hohenegger, C., Ilyina, T., Jahns, T., Jimenez-de-la-Cuesta, D., Jungclaus, J., Kleinen T., Kloster, S., Kracher, D., Kinne, S., Kleberg D., Lasslop G., Kornbluh, L., Marotzke, J., Matei, D., Meraner, K., ,U., Modali, K., Mobis, B., Muller, W.A., Nabel, J.E.M.S., Nam, C.C.W., Notz, D., Nyawira, S., Paulsen, H., Peters, K., Pincus, R., Pohlmann, H., Pongratz, J., Popp, M., Raddatz, T.J., Rast, S., Redler, R., Reick, C.H., Rohrschneider, T., Schemann, V., Schmidt, H., Schnur, R., Schulzweida, U., Six, K.D., Stein, L., Stemmler, I., Stevens, B., Storch, J., Tian, F., Voigt, A., Vrese, P., Wieners, K., Wilkenskjaeld, S., Winkler, A., Roeckner, E., Developments in the MPI-M Earth System Model version 1.2 (MPI-ESM1.2) and its response to increasing CO₂, *J. Adv. Model. Earth Syst.*, 2019, vol. 11, pp. 998–1038.
 29. Otto-Bliesner, B.L., Braconnot, P., Harrison, S.P., Lunt, D.J., Abe-Ouchi, A., Albani, S., Bartlein, P.J., Capron, E., Carlson, A.E., Dutton, A., Fischer, H., Goelzer, H., Govin, A., Haywood, A., Joos, F., LeGrande, A.N., Lipscomb, W.H., Lohmann, G., Mahowald, N., Nehrbass-Ahles, C., Pausata, F.S.R., Peterschmitt, J.-Y., Phipps, S.J., Renssen, H., and Zhang, Q., The PMIP4 contribution to CMIP6, Pt 2: Two interglacials, scientific objective and experimental design for Holocene and Last Interglacial simulations, *Geosci. Model Dev.*, 2017, vol. 10, pp. 3979–4003.
 30. Sidorenko, D., Rackow, T., Jung, T., Semmler, T., Barbi, D., Danilov, S., Dethloff, K., Dorn, W., Fieg, K., Goßling, H.F., Handorf, D., Harig, S., Hiller, W., Juricke, S., Losch, M., Schroter, J., Sein, D.V., and Wang, Q., Towards multi-resolution global climate modeling with ECHAM6-FESOM. Pt. I: Model formulation and mean climate, *Clim. Dynam.*, 2015, vol. 44, pp. 757–780.
 31. Volodin, E.M., Mortikov, E.V., Kostyryn, S.V., Galin, V.Y., Lykossov, V.N., Gritsun, A.S., Diansky, N.A., Gusev, A.V., Iakovlev, N.G., Shestakova, A.A., and Emelina, S.V., Simulation of the modern climate using the INMCM48 climate model, *Russ. J. Numer. Anal. M.*, 2018, vol. 33, pp. 367–374.

Translated by G. Krichevets